

# ANALYSIS OF PERFORMANCE OF THE ULTRA-THIN WHITETOPPING SUBJECTED TO SLOW MOVING LOADS IN AN ACCELERATED PAVEMENT TESTING FACILITY

*Sudarshan Rajan\**, *Jan Olek\** (corresponding author), *Thomas L. Robertson*, *Khaled Galal*<sup>+</sup>, *Tommy Nantung*<sup>+</sup> and *W. Jason Weiss*<sup>\*</sup>

*\* School of Civil Engineering, Purdue University, West Lafayette, IN 47907-1284, (Ph) 765-496-1364, e-mail: olek@ecn.purdue.edu*

*\*\*Electrical Engineering Technology, Purdue University*

*<sup>+</sup>Indiana Department of Transportation, Division of Research, 1205 Montgomery, P.O. Box 2279, West Lafayette, Indiana, 47906, (Ph) 765-463-1521.*

## ABSTRACT

Ultra-Thin Whitetopping (UTW) is rapidly emerging as a technology that can be used for the rehabilitation of deteriorated pavements. To investigate the performance of UTW when they are placed over flexible pavements and subjected to a slow moving load, four whitetopping mixtures were placed over a milled asphalt surface in the Accelerated Pavement Testing (APT) facility of the Indiana Department of Transportation (INDOT) Research Division in West Lafayette, Indiana in the Fall of 1999. This paper presents the response of the UTW to repeated loading, including analysis of stresses and strains, with the goal of identifying the factors influencing the performance of UTW. The data was analyzed to determine the maximum strains and their location, the degree of bonding between the UTW and the existing pavement, and the pavement performance under repeated loading. The study described in this paper is a part of a larger effort to develop preliminary design guidelines for UTW construction in Indiana including development of the semi-empirical model for performance prediction of UTW.

## INTRODUCTION

Ultra-Thin Whitetopping (UTW) is a relatively new pavement rehabilitation technique that is used mainly for the repair of deteriorated asphalt pavements. Typically, UTW is constructed by milling the distressed, top portion of the asphalt pavement, and placing a thin (not more than 104 mm (4") in thickness) concrete overlay on top of the milled surface. Based on U.S. experience, ultra-thin whitetopping can be defined as: "a concrete overlay 50 mm to 100 mm thick with closely spaced joints, bonded to an existing asphalt pavement" [1].

The first UTW project was completed in Louisville, Kentucky in September 1991 [2-5]. This experimental project included the construction of two concrete overlays (90 mm and 50 mm thick) on the access road to a waste disposal landfill. The access road serviced 400 to 500 trucks, 5 days in a week. This was viewed as a suitable site for the accelerated testing of the UTW pavement, as the truck loading was 20 to 100 times greater than that on an average low volume road. The success of this project led to a number of different projects in other states including Georgia, Tennessee, Virginia, Florida and Iowa [1].

One of the most recent research UTW projects was conducted by the Federal Highway Administration (FHWA) and the American Concrete Pavement Association (ACPA) at the Turner-Fairbanks Test Facility in McLean, Virginia [6]. The purpose of this study was to

evaluate design factors affecting the performance of the UTW. The main parameters to be analyzed were the UTW thickness and the required joint spacing, as a function of concrete mixture proportions and grades of HMA binder. An Accelerated Loading Facility (ALF) was used to test the lanes, which were instrumented with strain gages, Linear Variable Differential Transformers (LVDTs) and thermocouples (temperature sensors) to monitor the response of the UTW system. The deflection and strain data obtained from this FHWA project is currently being used to evaluate finite element and other types of response models for the UTW [6]. Other research projects of a similar nature have been undertaken at Ohio University, Kansas State University and University of Florida [7, 8].

## OBJECTIVE OF STUDY

The overall objective of the research described in this paper was to investigate the use of thin concrete overlays as a rehabilitation option for rutted asphalt pavements. The specific objective discussed in this paper deals with the evaluation of the state of strains and stresses in the UTW system exposed to slow moving heavy truck traffic. To achieve this, the overlay was instrumented with strain gages, thermocouples and LVDTs. This equipment was used to measure the pavement response to load and temperature. It is expected that the outcome of this research will be used to improve the existing empirical UTW design methods and will serve as a basis for the development of preliminary design guidelines for installation of UTW at intersections.

## EXPERIMENTAL FACTORS

### Accelerated Pavement Testing (APT) Facility

The APT Facility used in this study is housed in a 186 m<sup>2</sup> environmentally controlled building and consists of a test pit, a loading mechanism and control/monitoring equipment. The test pit measures 6.1 m x 6.1 m (20 ft x 20 ft) and is 1.83 m (6 ft) deep. The base of the pit consists of four 208 mm (8") thick concrete slabs (1.52 m (4.95 ft) wide) that are placed on top of 1.52 m (5 ft) thick layer of pea gravel which together form an extremely stiff subgrade. These slabs have internal rubber hoses through which water may be circulated to heat or cool the slabs. A 104 mm to 152 mm (4 to 6 inch) thick layer of asphalt or concrete may be placed on top of this configuration in one or more layers.

### Data Acquisition System

The data acquisition system used in this research was a System 6000 unit that was manufactured by Vishay Measurements Group. The system, as used in this research, consisted of a model 6100 scanner (holding up to 20 input cards), PCI hardware interface, and PC-based StrainSmart software. For each channel, data was recorded at the rate of 250 samples per second. In addition, the data acquisition system was equipped with high-range FIR filtering system allowed the background electrical noise of the testing apparatus to be filtered out.

### Experimental Set Up

For the purposes of the current project, it was decided to divide the APT test pad (6.1 m (20 ft) long and 6.1 m (20 ft) wide) into four test lanes (each 1.2 m (4 ft) wide) thus leaving a 0.6 m (2 ft) wide shoulder along the two sides of the test pad. In addition, for each lane, a 0.30 m (1 ft)

long strip was added at each end to accommodate the formwork for the construction of the concrete overlay. The resulting total length of the overlay for each lane was thus 7 m (22 ft). Based on the design parameters selected for this project (thickness of overlay, joint spacing, and type of concrete (plain vs. fiber reinforced)) and the limitation on having only four lanes, it was decided to construct the four lanes with two different thicknesses (2.5" and 4") and two different types of concrete (plain and fiber-reinforced as shown in Table 1). The joint spacing was kept constant at 1.2 m (4 ft) for all the lanes.

Table 1. Summary of the Material Types and Thickness Information for the Test Lanes

Lane Number	Material	Thickness
1	Plain concrete	104 mm (4")
2	Fiber-reinforced concrete	63.5 mm (2.5")
3	Plain concrete	104 mm (4")
4	Fiber-reinforced concrete	63.5 mm (2.5")

## CONSTRUCTION MATERIALS AND TESTING

The mixture proportions chosen for this study were based on information collected from the literature. The mixture proportions were selected to utilize fiber reinforcement, low water cement ratio ( $< 0.40$ ) and to achieve sufficient workability. Two types of mixtures were designed, one for plain concrete and one for the fiber reinforced concrete. The fiber reinforced concrete mix was very similar to the plain concrete mix except for the addition of 50/63 3M Polyolefin fibers. Table 2 shows the mixture composition of the UTW mixtures.

The samples cast included standard 104 mm by 208 mm (4" by 8") cylinders for compressive strength testing, 152 mm by 304 mm (6" by 12") cylinders for split tensile strength testing, and 152 mm by 152 mm by 533 mm (6" by 6" by 21") beams for third point flexural strength testing. The specimens were cast in accordance to the ASTM specification C192. After casting, the laboratory mixtures were covered with wet burlap and kept in molds for 24 hours. They were then demolded and cured in the moist room until the testing time. The samples prepared at the APT facility during the construction of the lanes were cured with wet burlap at ambient temperature for the first three days after which they were transported to the moist curing room in the laboratory.

The mechanical tests conducted on the concrete specimens included determination of compressive strength, split tensile strength and the flexural strength (using the third point-loading configuration). The concrete placed at the APT had a slump of 89 mm (3.5") for the plain concrete mixtures and a slump of 63 mm (2.5") for the fiber reinforced concrete mixtures. The Table 3 shows both the test results for concrete produced in the laboratory and for concrete produced at the APT facility.

Table 2. Concrete Mixture Compositions

Material	kg/m <sup>3</sup>	lb/yd <sup>3</sup>
Type I Cement	375	632
Class C Fly Ash	70	118
Coarse Aggregate (d <sub>max</sub> = 12 mm)	1000	1684
Natural Sand	750	1263
Water	160	270
HRWR Admixture	3-4 l/m <sup>3</sup>	2.3 – 3 liters/ yd <sup>3</sup>
3m 50/63 Polyolefin Fibers*	10 (0.45% v/v)	2.3 – 3 liters/ yd <sup>3</sup>

\*used in fiber-reinforced concrete mixture only

Table 3. Laboratory Mixture Test Results for Plain and Fiber Reinforced Concrete

Property	Age (Days)							
	1 Day		3 Day		7 Day		28 Day	
Plain Concrete								
	L	F	L	F	L	F	L	F
Compressive Strength (ASTM C39)	18.75	19.18	39.72	35.95	49.14	45.16	73.57	83.21
Split Tensile Strength (ASTM C496)	1.95	N/A	3.05	N/A	3.35	N/A	4.51	N/A
Flexural Strength (ASTM C78)	3.97	3.04	4.77	4.07	N/A	4.76	6.91	5.55
Fiber Reinforced Concrete								
	L	F	L	F	L	F	L	F
Compressive Strength (ASTM C39)	19.95	16.56	41.09	31.84	51.52	44.51	62.44	71.83
Split Tensile Strength (ASTM C496)	1.49	N/A	N/A	N/A	2.27	N/A	4.48	N/A
Flexural Strength (ASTM C78)	4.41	2.62	N/A	4.55	5.95	5.59	6.99	5.83

Notes: All results obtained from an average of 3 or 4 samples

All results in MPa.

L: Laboratory samples

F: Field samples (APT)

N/A: Test results not available

## UTW INSTRUMENTATION

The instrumentation installed in the slabs of the test lane included nine strain gages (3 transverse (T series) and 6 longitudinal (M and S series)) one or two strain gage rosettes (R series) and two LVDTs. In addition, three gages (S2 series) were also located in one of the slabs of the adjacent lane (i.e., non-loaded) lane. The specific location and the nomenclature for all gages for a typical test lane are shown in the Figure 1. Please note that in order to help with the identification of the locations of the sensors the panels in the test lanes were numbered consecutively starting with panel 1 which was adjacent to the starting point of the loading cycle as shown in Figure 1. The summary of gage nomenclature is shown in Table 4.

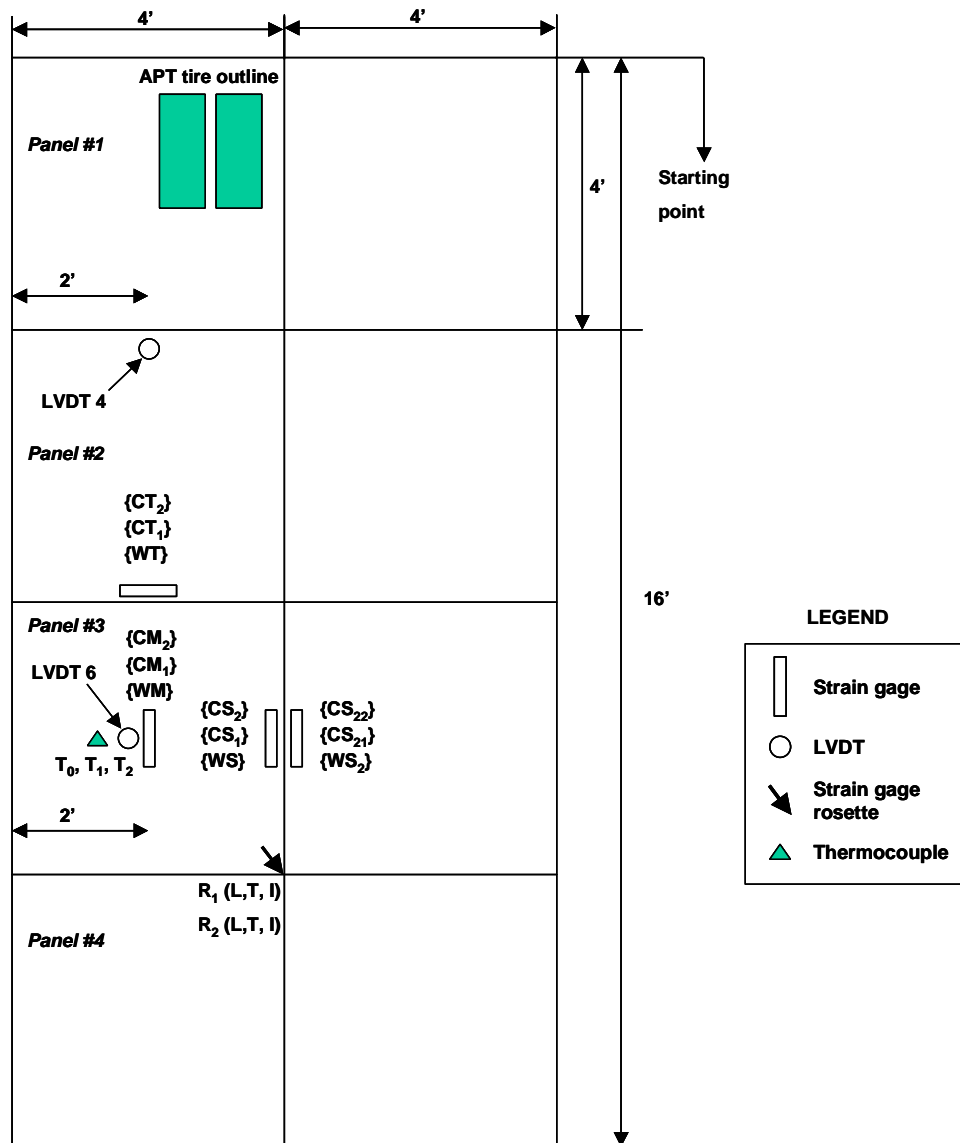


Figure 1. Plan view of the instrumentation layout for a typical test lane

Table 4. Summary of Gage Nomenclature

Lane	Type	Location	Depth or orientation
Could be 1,2 3 or 4	Concrete embedment gage ( <b>C</b> ) Non-encapsulated gage ( <b>W</b> ) Rosette at the corner ( <b>R</b> ) <b>L</b> : Longitudinal leg of the rosette <b>T</b> : Transverse leg of the rosette <b>I</b> : Inclined leg of the rosette	<b>M</b> : near the side of the mid panel <b>S</b> : Longitudinal joint of the loaded lane <b>S2</b> : longitudinal joint adjacent lane <b>T</b> : near the transverse joint	<b>1</b> : 12mm above the bottom of the UTW concrete overlay <b>2</b> : 12mm below the top of the UTW concrete overlay (All 'W' gages placed on milled HMA)

### TEST PLAN

The initial test plan called for testing of all lanes until signs of failure (i.e., cracking, faulting or debonding) could be detected. However, time constraints led to modifications that included increasing the wheel load and (for one of the lanes) increasing the temperature of the pavement in an effort to accelerate the damage in some cases (if any). The summary of the test plan is given in Table 5.

Lane 1 was loaded with 100,000 wheel passes. During the first 30,000 passes, the wheel load was 5.45 kN (12,000 lbs). However, for the remaining 70,000 passes, the wheel load was increased to 9.08 kN (20,000 lbs). This was done to observe whether the heavier loading had any effect on accelerating the damage to the pavement. After 100,000 passes, minimal damage was observed and the strains stabilized. As such the testing of Lane 1 was terminated after 100,000 passes. Based on the minimal changes in Lane 1 it was decided not to test Lane 2. Lane 3 was tested for 150,000 passes using only the lower load of 5.45 kN, since it was a thinner overlay. The performance of Lane 3 under this load was similar to the performance of Lane 1. Lane 4 was tested using a 9.08 kN load and after the initial 100,000 passes elevated temperature was used to accelerate the damage. The slabs were heated from below to a temperature up to 130°F and kept at this temperature for a period of 96 hours. The slabs were then cooled down to a temperature of 85°F and maintained at this temperature for a period of 96 hours. In total, two cycles of heating and cooling were applied to the overlay in the test lane 4. The following sections of the paper present the results obtained from the data analysis of Lane 1, 3 and 4.

Table 5. Schematic of the Lane Layouts and the Test Plan

Lane 1	Lane 2	Lane 3	Lane 4
4" Thick Plain Concrete	4" Thick Fiber Concrete	2.5" Thick Plain Concrete	2.5" Thick Fiber Concrete
Load of 12,000 lbs for first 30,000 passes Load of 20,000 lbs for next 70,000 passes Tested for a total of 100,000 passes	Was not tested	Load of 12,000 lbs for 150,000 passes	Load of 20,000 lbs for 250,000 passes Tested at elevated temperature after 60,000 passes 2 Cycles of heating and cooling (85-130°F)

## DATA ANALYSIS OF LANE 1

### Type and Format of Data

The data collected by the data acquisition system consisted of strains recorded from 4 sets of gages (with 3 gages in each set) and 2 sets of rosettes, deflections obtained from 2 LVDTs and temperature recorded by 3 thermocouples installed at various depths in the pavement. Initially, for each of the lanes tested, the data was scanned and recorded after every 200 passes of the wheel over the sensor. As the test progressed the frequency of recording was decreased to one in 500 passes and finally to one in 1000 passes. Synchronizing the clocks of the computer, which controlled the travel of the wheel carriage and that of the computer that ran the data acquisition system, enabled the real time recording of the instrumentation data by the system. The data was saved in the form of an ASCII text file, which could be opened by any standard spreadsheet program. The dynamic-load (under the moving wheel) strains were recorded by the strain gages, as the wheel was moving along the test lane. The term “dynamic-load strain” (as used in this paper) is defined as the strain magnitude at the particular gage location as the wheel moved over that particular point. The frequency of sampling for the gages was 250 Hz. This, when translated to the wheel moving at 8 km/h (5 mph) corresponds to one reading every 1.1 cm (0.44”) of the wheel traverse. The trends in dynamic-load strain indicate how the strains in the pavement changed at a particular gage location, as the wheel moves towards, passes over the gage and moves away from the gage. In addition to dynamic-load strains, permanent strains were recorded daily before the beginning of the test (with the wheel completely outside of the test lane). The trends observed in permanent (static) strains and deflections were used as indicators of permanent deformations accumulating in the pavement with increasing number of load repetition. The typical output data file included the strains, the deflections, the temperature data and the wheel position data that were recorded by different channels of the system. The strains were reported in microstrains, deflections and wheel position was recorded in inches and the temperature data in degrees Fahrenheit.

### Analysis of Dynamic-Load Strains

The analysis presented in this section includes the data collected during testing of Lane 1 up to a 100,000 passes. During the first 30,000 passes, the load applied to the wheel was 5.45 kN (12000 lbs). The load was then increased to 9.08 kN (20,000 lbs) for the remaining 70,000 passes. This section discusses the variations in dynamic-load strains during the first pass of the wheel and during the 100,000<sup>th</sup> pass of the wheel as recorded by both the longitudinal gages located in the wheel path and the gages located in the adjacent lane.

- a) Longitudinal gages at the edge of the longitudinal joint within the test lane.  
(1-C-S-1, 1-C-S-2, 1-W-S)

Figure 2 shows the typical response of all three gages as the wheel passes over it for the first time. This set of gages was located directly under the passing wheel. The top gage in concrete (1-C-S-2) shows a compressive strain and the bottom two gages (located at the bottom of concrete (1-C-S-1) and on the top of milled asphalt (1-W-S)), respectively, show tensile strains as the wheel passes directly on top of them. The strains recorded have a very low magnitude (of the order of about 10 microstrain). It can also be seen from the Figure 2 that as the wheel position approaches the gage location; the top of the panel experiences tensile strain and the

bottom of the panel experiences compressive strain. This could be because the panel curls upwards. As the wheel reaches the position directly on top of the gage, the strains quickly reverse and the top gage goes into compression while the bottom gage goes into tension indicating that, the panel curls downward under the wheel load. The strains reverse again as the wheel leaves the panel and moves on to the next panel. This phenomenon can be explained by the fact that there is a relative vertical motion of the pavement structure as the wheel moves from one panel to another. This relative movement causes a wave like deformation of the slabs. The schematic shown in Figure 3 represents the slab movement with respect to the wheel position.

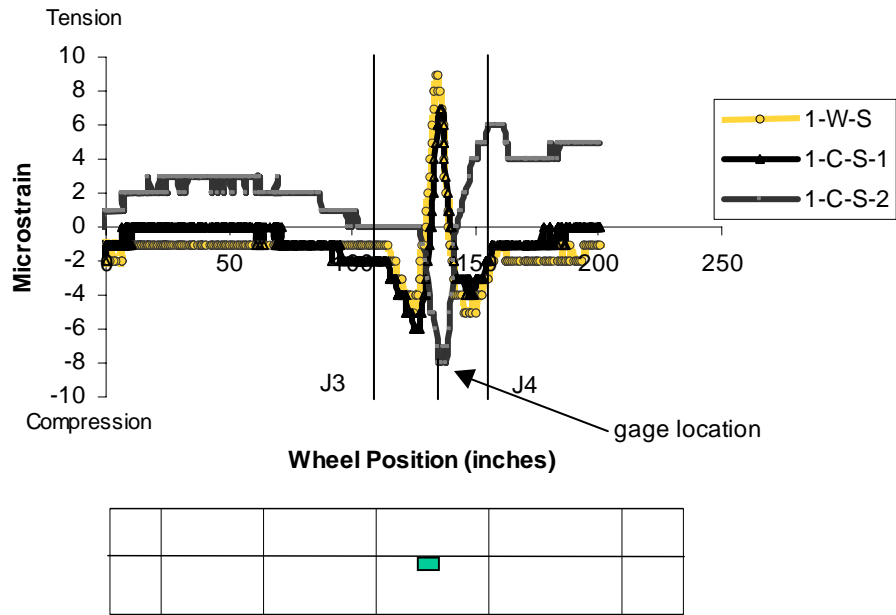


Figure 2. Typical strain response of edge longitudinal gages under the moving wheel during the first pass

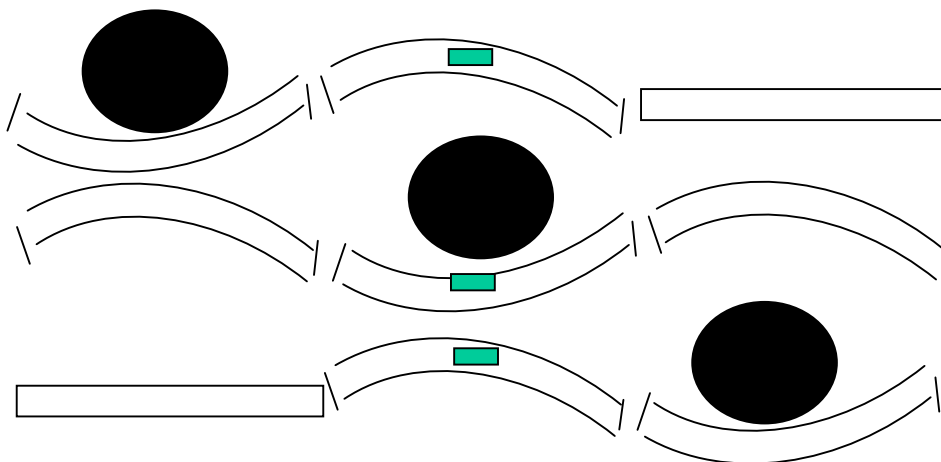


Figure 3. Relative motion of slabs causing reversal of dynamic-load strains

Figure 4 shows the longitudinal edge gages response during the 100,000<sup>th</sup> pass. The magnitude of strains created by the motion of the wheel over the lane is higher after 100,000 passes than it was during the first pass. The base strains have also increased which indicate formation of permanent strains in the pavement. The gage at the top of the concrete (1-C-S-2) shows a maximum dynamic-load compressive strain of 25 microstrain whereas the gages at the bottom of the concrete (1-C-S-1) and top of the asphalt (1-W-S) show a maximum dynamic-load tensile strain of 25 microstrains and 20 microstrains, respectively. The maximum strains recorded by the gages, due to the reversal phenomenon discussed above, are much greater in magnitude than the strains generated when the wheel load is directly on top of the gages. This was not observed during the first pass.

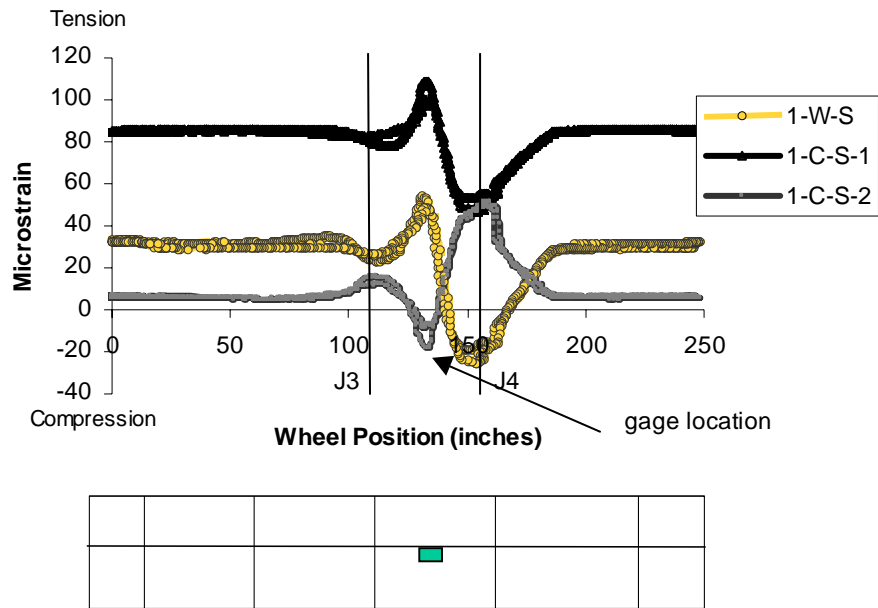


Figure 4. Typical strain response of edge longitudinal gages under the moving wheel during the 100,000<sup>th</sup> pass

- b) Longitudinal gages at the edge of the longitudinal joint in the lane adjacent to loaded test lane (1-W-S2, 1-C-S2-1, and 1-C-S2-2)

Unlike the response from the gages in the loaded lane, after the initial pass, the response in the gages located in the adjacent lanes does not follow a distinctive pattern. In general strains in the adjacent lane were low and scattered when the wheel load was 5.45 kN (12,000 lbs). However, when the load was increased to 9.08 kN (20,000 lbs), the gage at the top of the concrete showed a compressive strain and the gage at the top of the asphalt showed a tensile strain as the wheel passed over them (see Figure 5).

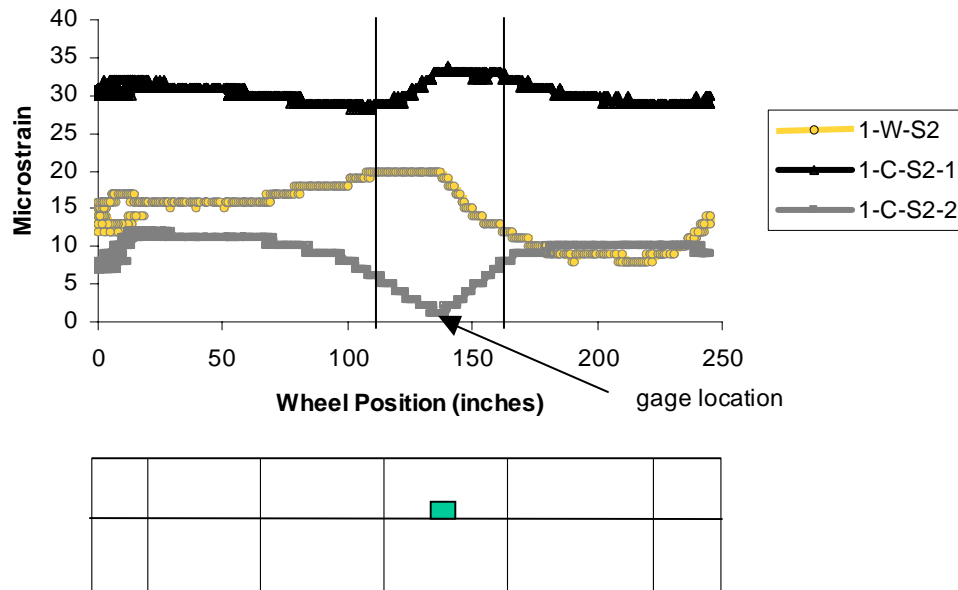


Figure 5. Dynamic-load strain of longitudinal edge gages in the adjacent lane during the 100,000<sup>th</sup> pass

#### Analysis of the Effect of Load Increase

The following sub-section discusses the effect of the load increase from 5.45 kN. (used for the first 30,000 passes) to 9.08 kN (used for the next 70,000 passes). The increase of the load caused an increase in the dynamic-load strains and deflections. The most noticeable changes were observed in the two sets of longitudinal gages located in the center and edge of the slabs. The dynamic-load strain increased almost two-fold. This increase was related to the increase in the load and was a linear function of the load. The changes recorded by the transverse gages and the rosettes, were very negligible and the average strain values remained low. The deflection recorded by the LVDTs was very small as well. Even after the load was increased to 9.08 kN, the deflection did not exceed 0.05” even after 100,000 passes.

In addition, the increase in the load caused the increase in the strains associated with the strain reversal phenomena discussed in the previous sections. The magnitude of this strain increased to almost about 4 to 5 times the strain value that was observed for the lower (12000 lbs) load. This indicates that the relative motion between the adjoining panels increased greatly with the increase of the load. This was mainly observed in the two sets of gages located at the center (M-series) and at the edge (S-series) of the panel. It could also be observed that the load increase resulted in the change of both the magnitude and the location of the critical (tensile) strain. The critical strain location shifted from the bottom of the slab to the top of the slab. The increase in magnitude is shown clearly by the data from the longitudinal edge (S-series) gages given in Figure 6.

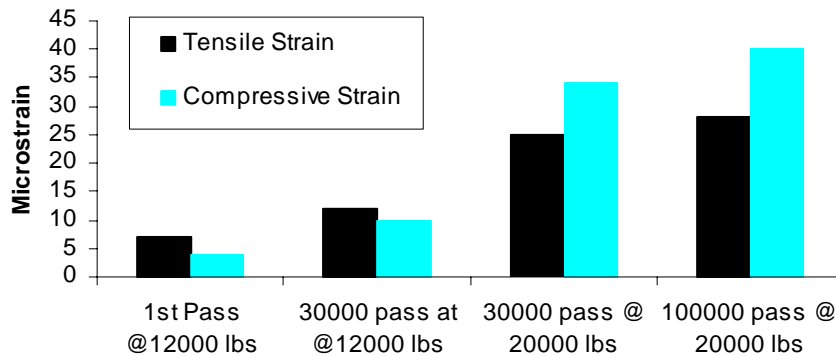


Figure 6. Change in maximum dynamic-load compressive and tensile strains (gage1-C-S-1) after increase in the load from 5.45 kN to 9.08 kN

#### Analysis of Permanent Strains

Initially lane 1 was loaded with 5.45 kN load (12,000 lbs) and it was observed that the strains increased with the number of passes. At 30,000 passes, the wheel load was increased from 5.45 kN to 9.08 kN (20,000 lbs). This caused an additional increase in the strain readings. In this sub-section, trends observed for permanent strains would be discussed. Lane 1 was tested at ambient (room) temperature. The maximum temperature gradient across the thickness of the slab was about 3°F. This corresponds to a maximum strain variation of about 15 microstrain (assuming linear coefficient of expansion for concrete to be  $5 \times 10^{-6}/^{\circ}\text{F}$ ). The strain variations near the bottom of the concrete overlay and at the top of the asphalt layer were higher than this value, suggesting that permanent strains were accumulating in the pavement due to repeated load applications. However, the increase could also be attributed to the fact that the wheel load was increased to 9.08 kN after the first 30,000 passes for the remaining test. The increase in wheel load and the increase in the number of load repetitions can not be isolated from each other in discussing the effects of the permanent strains and deflections and the extent to which each of these is affecting the fatigue damage of the pavement can not be determined quantitatively. Figure 7 shows the permanent strain variation in the gages located in the center of panel 3 in lane 1. The strains at the bottom of the concrete (1-C-M-1) and the top of the asphalt layer (1-W-S) increase with the increase in the number of passes. The strains on the asphalt layer however tend to stabilize after 70,000 passes. There is not much change in the strains at the top of the concrete (1-C-M-2).

Figure 8 shows the comparison of permanent strains at the top and bottom of the concrete overlay for gages located in both the test lane as well as the adjacent lane. It can be observed that the trends in the permanent strains in the longitudinal gages installed in both the test lane as well as the adjacent lane are very similar. The magnitude of the strains in the top of the concrete is almost equal for both sets of gages. However, the strains at the bottom of concrete are higher for the gage located in the test lane. This may be attributed to the fact that the gage in the test lane was subjected to the wheel load more directly than the gage in the adjacent lane.

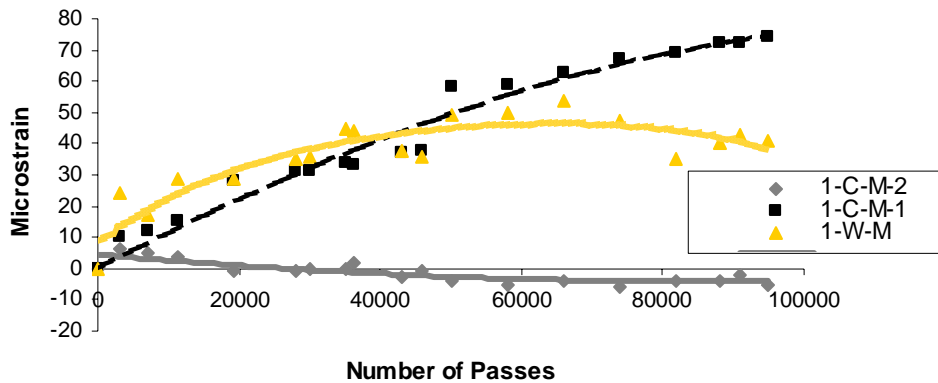


Figure 7. Variation of longitudinal mid-panel strain with number of passes

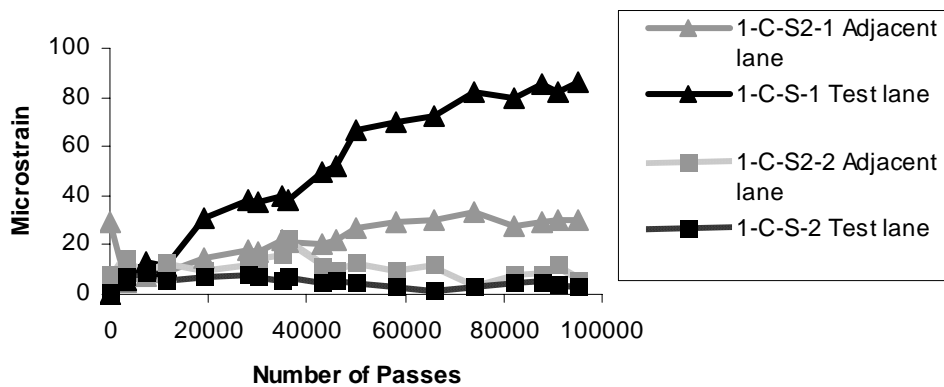


Figure 8. Comparison of permanent strains at the top and bottom of the concrete overlay in longitudinal gages in the test lane and the adjacent lane

### DATA ANALYSIS OF LANE 3

#### Analysis of dynamic-load strains

The strains and deflections produced in lane 1 were low. It was therefore decided to test the thinner overlay to observe the effects of accelerated loading on it. After the test of the 100 mm (4") thick overlay in lane 1 was completed, the loading wheel was moved to lane 3 to test the 63 mm (2½") thick overlay. Due to the reduced thickness of the overlay, it was decided to use the lower (5.45 kN) load during the entire testing period. This section discusses the variations in dynamic-load strain during the first and the 100,000<sup>th</sup> pass of the wheel as recorded by the longitudinal gages located in the wheel path.

- a) Longitudinal gages at the edge of the longitudinal joint within the test lane (3-C-S-1, 3-C-S-2, 3-W-S)

The data recorded by the gages at the edge of the longitudinal joint in lane 3 during the first pass of the wheel are shown in Figure 9. The top gage in concrete (3-C-S-2) was found defective at the beginning of the test and did not register any strains. The bottom gage in concrete (3-C-S-1) and the gage at the top of milled asphalt (3-W-S) show tensile strains as the wheel passes directly on top of them. These gages show a compressive strain, just before the wheel passes exactly on top of the gage. This is similar to the response of the corresponding gages in lane 1. However, the reversal immediately after the wheel passes over the gage is not as pronounced as that in lane 1. The strains recorded by both gages were very similar in magnitude, the gage at the asphalt (3-W-S) showing a slightly higher strain value than the gage at the bottom of the concrete (3-C-S-1). Figure 10 shows the gage response of the above gages at the 100,000<sup>th</sup> pass. The dynamic-load strains did not change very much after 100,000 passes and were very similar in magnitude to the ones shown in Figure 9. The slight shift in the base values could be attributed to the effect of temperature gradient on the strains.

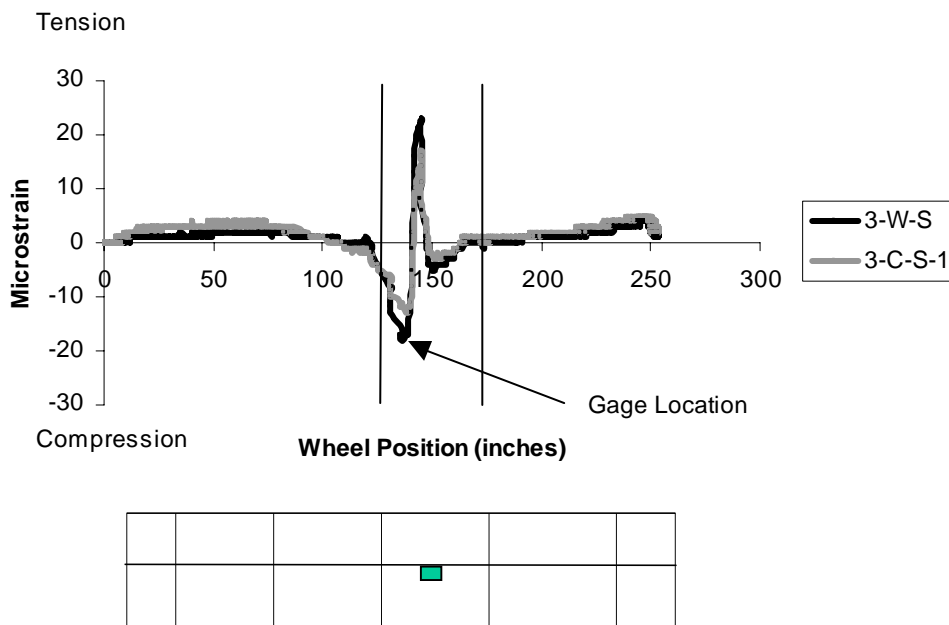


Figure 9. Strain response of edge longitudinal gages under the moving wheel during the first pass

Figure 11 shows the magnitudes of the maximum dynamic-load tensile and compressive strains recorded by the gage at the bottom of the concrete. The magnitudes of the strains are almost constant with the increasing number of repetitions of the wheel loads. The tensile strains show a slight decrease after 50,000 passes. The dynamic-load compressive strain however exceeds the tensile strain, which indicates the accentuated effects of the strain reversal discussed in the previous sections.

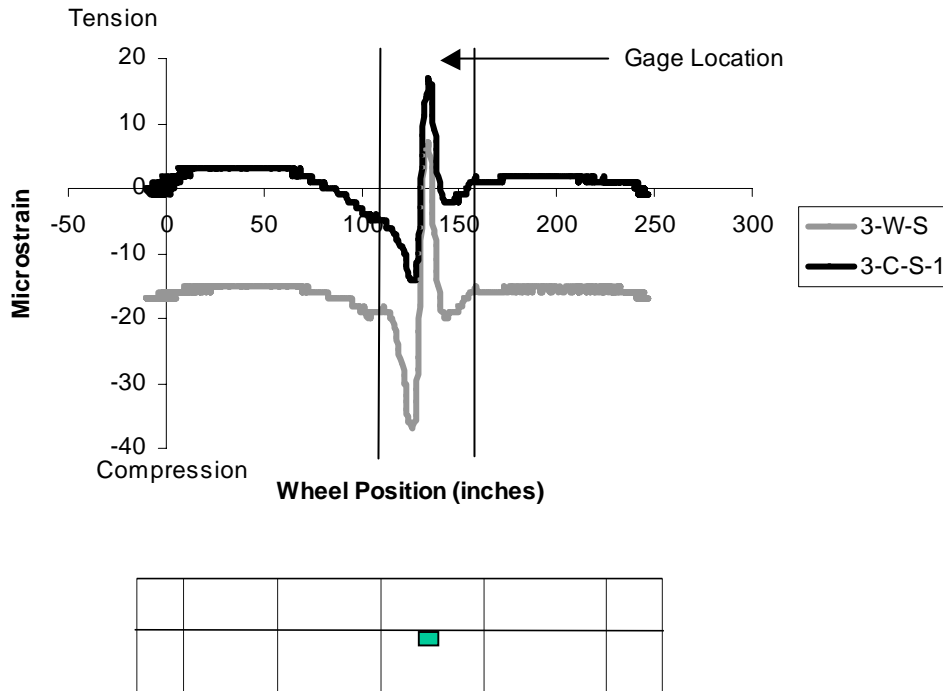


Figure 10. Strain response of edge longitudinal gages under the moving wheel during the 100,000<sup>th</sup> pass

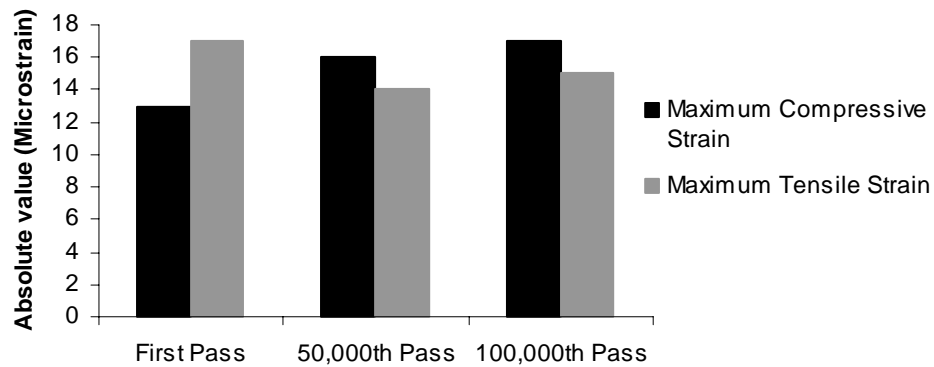


Figure 11. Change in maximum dynamic-load compressive and tensile strains in gage 3-C-S-1 (located at the bottom of the concrete overlay)

## DATA ANALYSIS OF LANE 4

After testing lane 3 at 5.45 kN, it was decided to test lane 4 under the increased load of 9.08 kN. This was because the strains and deflections produced in lane 3 were very low and the effect of repeated loading did not cause much distress to the pavement. Lane 4 was tested at ambient temperature for the first 100,000 passes. Since this loading did not cause much increase in strains, it was decided to increase the temperature of the slab to accelerate potential distress of the pavement. The following sections discuss the elevated temperature testing of lane 4 and the variation of dynamic-load strains during this testing.

### Elevated temperature testing

The increase in the temperature of the pavement was accomplished by circulating hot water through the network of pipes installed under the pavement. The heating continued until the pavement reached the temperature of 130°F. The loading also continued while the pavement was being heated. Thus by the time the temperature reached 130°F, 140,000 passes of wheel load had been applied to the pavement. The heating was then turned off for the next 20,000 passes. During this time, the temperature of the pavement dropped to about 95°F. After 160,000 passes, the heating was turned on again and remained on until 200,000 passes was reached. The heating was then turned off again. This procedure resulted in two cycles of heating and cooling that were applied to lane 4. The temperature was monitored using three thermocouples located one on top of the other at different depths in the overlay. The bottom thermocouple was placed on the milled asphalt surface, and the top two thermocouples were located 18 mm from the top and bottom of the concrete overlay, respectively. The temperature variation with the number of passes is shown in Figure 12.

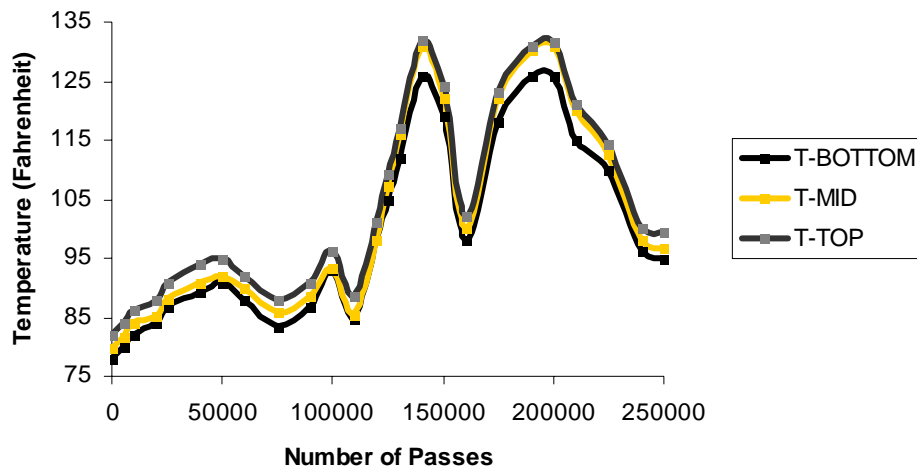


Figure 12. Temperature variation in lane 4

### Analysis of Dynamic-Load Strains

- a) Longitudinal gages at the edge of the longitudinal joint within the test lane (4-C-S-1, 4-C-S-2, 4-W-S)

The response of these gages after the first pass is shown in Figure 13. It can be observed that this response is similar to the response of the corresponding gages in the other two previously described lanes (1 and 3). The gages showed a strain reversal both before and after the wheel passed over the gage location. This was especially pronounced in the gage located on the asphalt surface (4-W-S). The initial dynamic-load strains were higher than those observed in lane 3 because of the application of 9.08 kN wheel load.

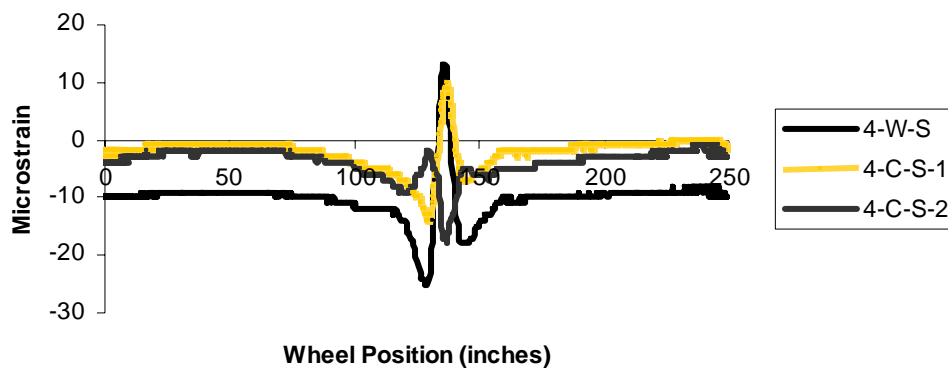


Figure 13. Dynamic-load strain response in longitudinal edge gages during the first pass

Figure 14 shows the variation of the dynamic-load strains at the top of the asphalt surface (recorded by gage 4-W-S) at the edge of the longitudinal joint. The dynamic-load strains for the gages have been represented only by the absolute values of strain (the negative sign associated with compressive strain has been discarded). As shown in Figure 14, the departure of the strain values from the base value occurs at about 110,000 passes. The dynamic-load strains increased considerably with increase in the temperature of the slabs subjected to the load of 9.08 kN. The strain reversal was also accentuated due to the increase in the slab temperature. The second peak in Figure 14 indicates this point, as the maximum compressive strain (caused by strain reversal) is greater than the maximum dynamic-load tensile strains.

Figure 15, shows the dynamic-load strain variation for the gage at the top of the slab located at the edge of the longitudinal joint (4-C-S-2). By comparing the curves shown in Figure 15 and the temperature variation shown in Figure 12, it can be observed that the trend in the strains follows the trend in the temperature variation. As the temperature increased, the values of the dynamic-load strains also increased and vice a versa. The dynamic-load tensile strain shown by this gage exceeds the dynamic-load compressive strain after the number of passes corresponding to the first and second heating cycles. As a result, the critical strain in the slab shifts from the

bottom of the slab to the top of the slab due to the increase in the dynamic-load tensile strain at the top.

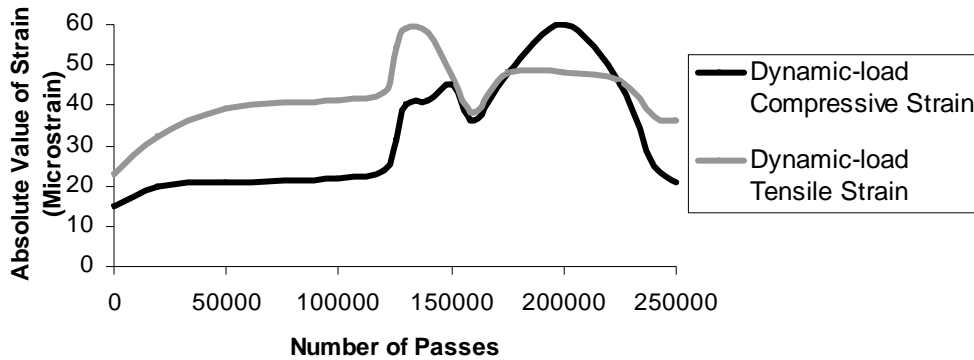


Figure 14. Variation of dynamic-load strains in gage 4-W-S (gage located on the milled asphalt surface) with number of passes

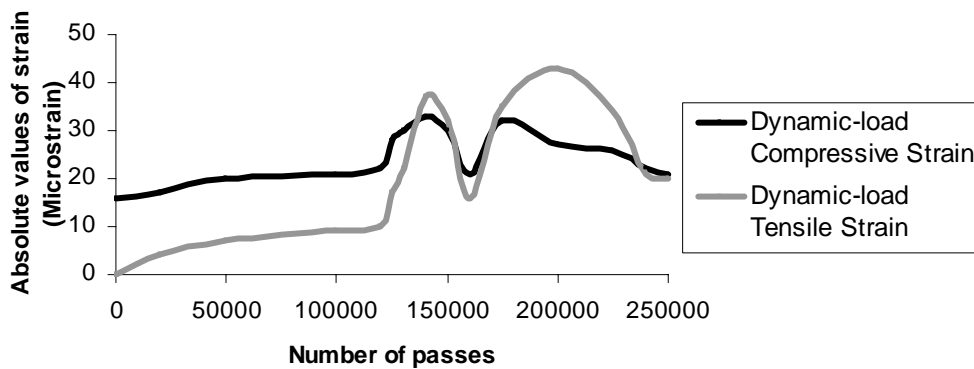


Figure 15. Variation of dynamic-load strain in 4-C-S-2 (gage located at the top of the concrete overlay) with number of passes

#### Analysis of permanent strains

The variation of the permanent strains detected by the longitudinal edge gages with the number of wheel passes is seen in Figure 16. The strains generated by the increase in the temperature of the slab did not disappear when the temperature of the slab was lowered. The strains on the asphalt surface were the highest among all strains that were recorded using the sensors. This can be explained by the fact that asphalt has higher temperature sensitivity (related to coefficient of

thermal expansion) and therefore deforms more due to temperature than concrete. For the gages at the longitudinal edge (as seen in Figure 16) the asphalt surface gage recorded a maximum strain of over 420 microstrains, whereas the gages in concrete showed values of around 120 microstrain and 50 microstrain at the bottom and top of the overlay, respectively. A significant increase in the permanent strains occurred at the time when the temperature of the slab was increased indicating that the permanent strains were affected more by the temperature increase than by the number of loading cycles.

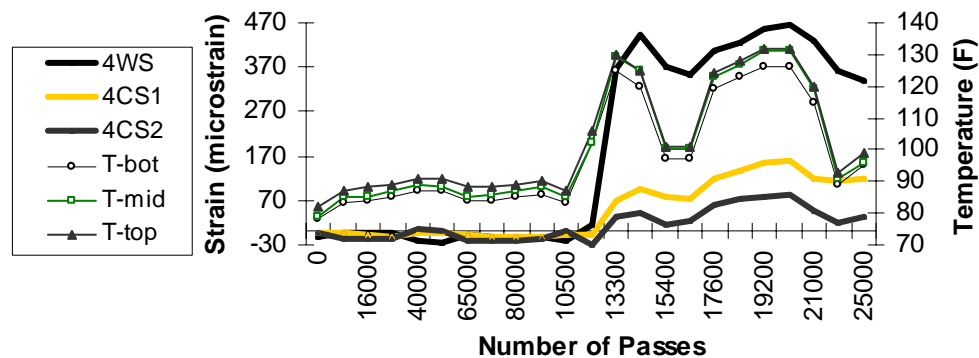


Figure 16. Temperature and permanent strain variation for longitudinal edge gages in Lane 4

## CONCLUSIONS

Based on the test results presented, the following conclusions can be drawn:

- The performance of all the UTW overlay sections tested was very satisfactory. The 100 mm (4") thick overlay exposed to two levels of load (5.45 kN and 9.08 kN) did not develop any significant strains or deflections even after 100,000 passes. The 63 mm (2.5") thick overlay in lane 3 also performed very well under the wheel load (of 5.45 kN) as no permanent deflections and strains accumulated after 150,000 passes of the loading wheel. The 63 mm (2.5") thick overlay in lane 4 exposed to 250,000 repetitions of the heavier wheel load (of 9.08 kN) and elevated temperature effects did not experience any structural damage.
- From the results of the accelerated pavement test, it could be concluded that the joint spacing of 1.2 m (4') in all the lanes was sufficient.
- The measured strains in the overlay were relatively proportional to the applied load. This suggests that the pavement response was linear within the overlay. The increase of temperature in lane 4 however affected the linearity of the pavement response, and the strains at the asphalt surface increased considerably because of the temperature gradient.
- Measurements of dynamic-load longitudinal strains indicated that the concrete overlay experienced significant stress reversal as the wheel rolled over the pavement. As the wheel approached given point in the pavement, the top and the bottom of the overlay

experienced a tensile and compressive strain respectively. When the wheel was exactly over the point, the strains quickly reversed causing the top of the slab to be in compression and the bottom to be in tension. These strains again quickly reversed as the wheel moved away from the given point.

- e) The dynamic-load strain measurements indicated the existence of a sufficient bond between the overlay and the underlying asphalt. It was also observed that the overlay thickness and the asphalt stiffness significantly affect the strains because of their influence on the location of the neutral axis.

#### ACKNOWLEDGEMENTS

This research was supported by the Indiana Department of Transportation (INDOT) through the Joint Transportation Research Program (JTRP) at Purdue University. The study was conducted at the Accelerated Pavement Testing Facility (APTF) at the Division of Research of INDOT in West Lafayette, Indiana. Their generous support is gratefully acknowledged. The technical assistance offered by Mr. Calvin Reck, technician at the APTF, is deeply appreciated.

#### REFERENCES

1. Cole, L.W., "Pavement Condition Surveys of Ultrathin Whitetopping Projects", *Proceedings Sixth International Conference on Concrete Pavements, Volume 2*, November 1997, Purdue University, West Lafayette, Indiana, pp. 175-187.
2. Mack, J.W., Cole, L.W., and Moshen, J.P., "Analytical Considerations for Thin Concrete Overlays on Asphalt", *Transportation research record 1388*, TRB, National Research Council, Washington D.C., 1993, pp. 167-173
3. Armaghani, J.M., and Tu, D., "Evaluation of Ultra-Thin Whitetopping in Florida", *Paper for presentation at Transportation Research Board*, National Council, Washington, D.C., 1996, pp. 15-20.
4. Cole, L.W., "Performance of Ultrathin Whitetopping Roadways" *Proceedings of the Conference American Society of Civil Engineers*, May 1999, Cincinnati, Ohio, pp. 583-590.
5. Cole, L.W., Mack, J.W., Packard, R.G., "Whitetopping and Ultrathin Whitetopping-The US Experience", *Proceedings American Concrete Pavement Association (ACPA)*, Skokie, Illinois, Volume 36, Number 2, pp.247 – 263
6. Cole, L.W., Sherwood, J., and Qi, X., "Accelerated Pavement Testing of Ultrathin Whitetopping", *Proceedings of the International Conference on Accelerated Pavement Testing*, October 1999, Reno, Nevada, Paper number CS1c (b), 18 p.
7. Armaghani, J.M., and Tu, D., "Rehabilitation of Ellaville Weigh Station with Ultra-Thin Whitetopping", *Transportation research record 1654*, TRB, National Research Council, Washington D.C., 1999, pp. 3-11.

8. Edwards, W.F., and Sargand, S.M., "Response of an Ultra-Thin Whitetopping Pavement to Moving Wheel Loads", *Proceedings International Conference on Accelerated Pavement Testing*, October 1999, Reno, Nevada, Paper Number CS1-4, 13 p.